

IberFire - a detailed creation of a spatio-temporal dataset for wildfire risk assessment in Spain

Julen Ercibengoa Calvo^{1, 2}, Meritxell Gómez-Omella¹, and Izaro Goienetxea Urkizu²

¹Tekniker, Spain, {julen.ercibengoa, meritxell.gomez}@tekniker.es

²UPV/EHU, jercibengoa001@ikasle.ehu.eus, izaro.goienetxea@ehu.eus

Abstract

Wildfires pose a critical environmental issue to ecosystems, economies, and public safety, particularly in Mediterranean regions such as Spain. Accurate predictive models rely on high-resolution spatio-temporal data to capture the complex interplay of environmental and anthropogenic factors. To address the lack of localised and fine-grained datasets in Spain, this work introduces *IberFire*, a spatio-temporal datacube at $1 \text{ km} \times 1 \text{ km} \times 1\text{-day}$ resolution covering mainland Spain and the Balearic Islands from December 2007 to December 2024. *IberFire* integrates 260 features across eight main categories: auxiliary features, fire history, geography, topography, meteorology, vegetation indices, human activity, and land cover. All features are derived from open-access sources, ensuring transparency and real-time applicability. The data processing pipeline was implemented entirely using open-source tools, and the codebase has been made publicly available. This work not only enhances spatio-temporal granularity and feature diversity compared to existing European datacubes but also provides a reproducible methodology for constructing similar datasets. *IberFire* supports advanced wildfire risk modelling through Machine Learning (ML) and Deep Learning (DL) techniques, enables climate pattern analysis and informs strategic planning in fire prevention and land management. The dataset is publicly available on Zenodo to promote open research and collaboration.

1 Background & Summary

Forest fires constitute a critical environmental issue with severe ecological, social, and economic implications. Wildfires not only destroy vast forest areas, cause the loss of natural habitats, and release large amounts of carbon dioxide; they can also cause substantial economic damage through the destruction of infrastructure, housing, and productive land.

Spain is one of the most affected countries within the European Union [1, 2]. Nearly 40% of the total burned area in the entire Mediterranean region of Europe between 1980 and 2008 was in Spain [3]. Furthermore, data from the European Forest Fire Information System (EFFIS) [4] indicate that over 7,000 fires have occurred in Spain since 2008, as can be seen in the left image of Figure 1.



Figure 1: Left: wildfires that occurred from 2008 to 2024, according to data from EFFIS. Right: selected area of interest to build the datacube.

Wildfires are progressively increasing in scale, with a growing number of autonomous communities experiencing wildfires spanning areas of 5,000 ha, 10,000 ha, and even 20,000 ha [5]. The year 2022 marked the most severe wildfire season, with two consecutive forest fires jointly burning over 60,000 ha, an area roughly equivalent to that of Madrid.

In this context, the development of precise predictive models can help with prevention and fire service management by providing early warnings and identifying high-risk areas. Physical models, such as the Canadian Fire Weather Index [6], leverage meteorological data and physical equations to make predictions; however, recent studies have shown that data-driven models often achieve superior performance in terms of predictive accuracy [7, 8].

Building Machine Learning (ML) and Deep Learning (DL) models for fire risk assessment requires high-resolution spatio-temporal features. Many data sources are available for this purpose: the Corine Land Cover (CLC) [9] dataset provides a classification of the land usage, ERA5-Land [10] offers hourly meteorological curated data and vegetation indices can be retrieved from the Copernicus Land Monitoring Service (CLMS) [11]. When complemented with additional variables, these data enable the development of robust fire-risk prediction models. However, these sources differ significantly in spatial and temporal resolution, format, and update frequency, making direct integration a non-trivial task.

Datacubes are multidimensional data structures designed to standardise spatial and spatio-temporal features with varying original resolutions, providing a consistent and accessible means of analysis. They facilitate the modelling of complex spatio-temporal phenomena without the need for separate pipelines for each data source. In the context of wildfire risk prediction, datacubes are particularly crucial, as they enable the integration of heterogeneous environmental variables that influence fire behaviour, like the CLC dataset and ERA5-Land, alongside historical fire records.

To the best of current knowledge, only two datacubes that include Spain within their area of interest are available for this purpose, although neither is specifically focused on the Spanish territory. On the one hand, *SeasFire Cube* [12] offers 59 variables from 2001 to 2021 with 0.25° spatial resolution (approximately 27 km at the equator) and 8-day temporal resolution. While this dataset may be used for fire-risk predictions, it is suggested that its resolution is not sufficiently granular for practical applicability at the scale of Spain. On the other hand, *Mesogeos* [13] offers a 1 km spatial resolution covering the Mediterranean area from 2006 to 2022, with 27 spatio-temporal features. In this case, it is believed that incorporating a broader range of Spain-specific features could enhance forest fire risk predictive models, potentially improving the accuracy of the predictions.

The *IberFire* [14] datacube was constructed to address this gap, a $1\text{km} \times 1\text{km} \times 1\text{-day}$ high-resolution datacube covering Spain from December 2007 to December 2024 with 260 different features related to forest fire risk. All features were selected based on their potential to be automatically retrieved from external sources, allowing for real-time model deployment.

The features of *IberFire* can be divided into 8 main categories: **auxiliary features** that help locate the cells, **fire history** obtained from EFFIS, **geographical location information** features, **land usage** from Copernicus Corine Land Cover [9], **topography variables** obtained from the European Digital Elevation Model [15], **human activity** related features retrieved from WorldPop[16] and OpenStreetMap [17], **meteorological variables** obtained from ERA5-Land [10], and **vegetation indices** downloaded from Copernicus Land Monitoring Service [11].

This paper presents two main objectives. The first is the introduction and public release of the *IberFire* datacube, which improves upon existing datasets in terms of resolution and feature diversity for Spain. The *IberFire* datacube offers high-resolution modelling capabilities to gain insights not only into Spain’s fire risk behaviour but also into climate-change pattern time-series modelling. The second objective is the provision of a reproducible, systematic methodology for constructing similar datacubes, an approach that can be extended to model other spatio-temporal environmental phenomena. This includes a detailed explanation of the generation of *IberFire*, along with the concepts needed to manipulate geospatial data.

1.1 Concepts and tools about Geographic Information Systems (GIS)

Geographic features are not usually stored in commonly used formats such as CSV (Comma Separated Values); instead, specific formats that contain integrated geographical coordinates, such as *raster* data, are used. Among these, *datacubes* organise spatial and temporal information into structured, multi-dimensional arrays. This structure enables efficient storage, retrieval, and analysis of geospatial variables over both space and time, since any cell of the grid can be accessed and every feature value of that cell can be retrieved. The construction of such a datacube requires an understanding of Geographic Information Systems (GIS). This section provides an introduction to GIS,

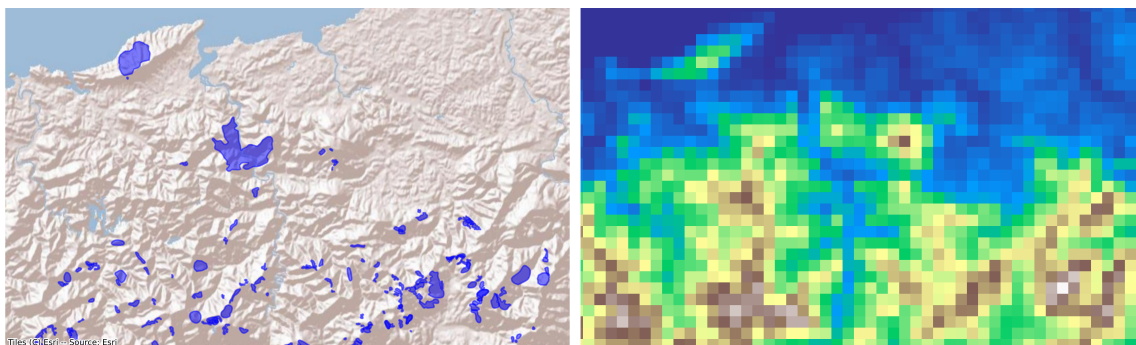


Figure 2: Left: Example of vectorial data (blue), some burned areas retrieved from EFFIS. Right: Example of raster data, elevation values on the same region as the left plot at a $1\text{km} \times 1\text{km}$ resolution.

emphasising the main data formats and processing techniques involved in manipulating spatial data.

Geographic Information Systems comprise a wide range of tools and data formats specifically designed for the storage, management, and visualisation of spatially-referenced data. In GIS, data are primarily represented using two distinct formats: vector and raster.

Vector data represents geographic features using points, lines, and polygons, which accurately capture geometric locations and boundaries [18]. Each instance of a vector dataset corresponds to a geographic shape with some feature values assigned. This representation is particularly suited for discrete features such as roads or specific fire-affected areas, as exemplified in the left image of Figure 2.

On the other hand, raster data represents geographic space as a regular grid of cells [19], where each pixel is assigned a value corresponding to a property of the geographic area, as can be seen in the right image of Figure 2. This data format is commonly used to represent continuous geographic phenomena such as climate data.

Interpolation methods are commonly used to adjust the resolution of raster data when homogenising datasets, a process known as *resampling*. For instance, this process can involve converting data from a finer spatial resolution, such as $100\text{m} \times 100\text{m}$, to a coarser resolution, like $1\text{ km} \times 1\text{ km}$. One widely used interpolation technique is the nearest neighbour interpolation, which assigns the value of the closest input cell to the output cell. Another resampling technique is average resampling, which computes the mean of all input cells that fall within the extent of each output cell.

Geographic data, whether in vector or raster format, relies on Coordinate Reference Systems (CRS). A CRS provides a standardised framework for accurately representing locations on the Earth’s surface. Different CRSs are designed to minimise spatial distortion, depending on the specific geographic area and the purpose of the analysis. For instance, the WGS84 CRS (also known as EPSG:4326), which is based on latitude and longitude, is often used for global analysis. In contrast, ETRS89-LAEA (also known as EPSG:3035) can be used for analysis based in Europe since it uses metres as units.

Downloaded GIS data may come in different CRSs, therefore, it is essential to transform all datasets to a common CRS, a process known as *reprojection*. In this study, all spatial layers were reprojected to the EPSG:3035 coordinate system, which is particularly suited for European spatial analyses due to its equal-area properties. However, individual CRS transformations applied during the preprocessing stage are not detailed, as they follow standard reprojection procedures widely adopted in geographic data processing.

Effectively processing geospatial data often requires the use of specialised tools. QGIS [20] is an open-source software employed for working with vector and raster data. This software offers an extensive set of functions for visualising, manipulating, automatically reprojecting, and resampling spatial datasets. Other tools for working with GIS data include the `rasterio` and `xarray` Python libraries, which provide modules for resampling raster data and creating datacubes, respectively. In this work, both QGIS and Python-based tools were employed, ensuring the reproducibility of the entire process through open-source software solutions.

Datacubes

In GIS, datacubes are essentially raster arrays stacked one on top of the other across time. Hence, for every timestamp, there is one raster representing the values of a specific feature at that timestamp.

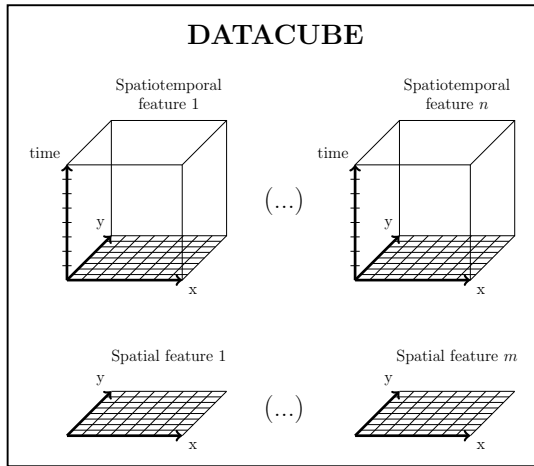


Figure 3: Visual representation of a datacube.

The rasters share the same CRS, coordinate values and resolution, hence, the only thing that differ are the values of the feature. For every feature a datacube contains, there is a set of stacked raster arrays; and the combination of all the features creates a datacube.

As some features do not vary over time, in order not to store repeated values, they can be saved as spatial-only features; hence, only one array for the entire period that the datacube covers. For instance, elevation values could be stored as spatial-only features. Figure 3 provides a visual representation of the datacube concept.

IberFire comprises 1188 x coordinates, 920 y coordinates and 6241 timestamps (t or time), one every day. For each (x, y, t) cell, a vector with all the feature values on that specific cell can be retrieved. The values of the retrieved spatial-only features will remain constant if the value of t is changed but (x, y) values do not vary. And the values of the retrieved spatio-temporal features will change if t changes, even if (x, y) remains constant. As an example, elevation does not vary even if t changes, but temperature, stored as a spatio-temporal feature, varies from day to day.

2 Methods

The creation of a *datacube* involves several steps. First, the spatio-temporal extent and resolution should be defined, which is influenced by the required granularity for the problem, the available computational resources, and the inherent resolution of the data to be employed. Once the spatio-temporal grid has been generated, the desired features should be downloaded and incorporated into the *datacube*. This is the most time-consuming stage, as it is highly feature-specific and requires the careful curation and integration of each variable. To achieve this, data are usually reprojected to a different coordinate reference system, interpolated, and combined.

This chapter provides a detailed analysis of the construction process of the *IberFire* datacube. Section 2.1 describes the generation of the spatio-temporal grid. After that, Section 2.2 analyses the auxiliary features introduced to the datacube. Then, Section 2.3 presents a thorough explanation of the integration of the primary output feature, `is_fire`. Subsequently, Sections 2.4 to 2.9 describe the incorporation of the explanatory variables into the dataset. Finally, Section 2.10 provides a summary of all external sources utilized in the construction of the datacube.

2.1 Grid generation

Given that datacubes are many equal-shaped raster arrays arranged along the time dimension, the grid of a datacube is required to be rectangular. A key consideration in the creation of the grid was ensuring that each cell represented exactly 1 km^2 of area. To achieve this, the grid was created on the EPSG:3035 CRS, whose units are meters. This approach ensures that all cells have the same importance and no cell is underrepresented. Within QGIS, the region of interest shown in the right image of Figure 1 was selected, and an empty base raster file with a $1 \text{ km} \times 1 \text{ km}$ spatial resolution was generated on that region. This empty raster file was then saved as a reference for the subsequent generation of the datacube and the creation of all the layers it contains.

The datacube was then constructed in Python using the `xarray` package. To build a datacube, it is necessary to define coordinates in each dimension, hence, for x , y , and t dimensions. Each coordinate consists of a vector of values that are used to locate the individual grid cells. These coordinates are similar to indices, but they can be any ordered set of values, including temporal sequences such as dates.

The base raster file’s horizontal and vertical coordinate values served as the coordinates of the x and y dimensions of the datacube respectively. Then, for the temporal dimension, the coordinates consisted of daily timestamps from 01/12/2007 to 31/12/2024. The final datacube comprised 1188 values for the x dimension, 920 values for the y dimension, and 6241 values for the time axis. As a result, the datacube contains a total of $1188 \cdot 920 \cdot 6241 \approx 6.8 \cdot 10^9$ different cells, each storing different features.

One important remark is that when adding new features to the datacube, it is possible to select the dimensions that affect the feature. For example, a feature that remains constant over time would only require the x and y dimensions, excluding the time axis, as represented in Figure 3. This approach prevents redundant storage of repeated values for time-invariant features.

2.2 Auxiliary features

After constructing the empty datacube, three auxiliary features were added to the dataset: `x_index`, `y_index`, and `is_spain`. These features, as analysed in Chapter 3, are not intended to serve as explanatory variables, but instead facilitate the manipulation and processing of the datacube.

The first two auxiliary variables, `x_index` and `y_index`, were introduced to facilitate the identification of grid cells. The `x_index` variable consists of a sequence of integer values representing the horizontal index of each cell, ordered from left to right. Similarly, the `y_index` indicates the vertical index, ordered from top to bottom. These auxiliary variables are particularly useful when individual cell values are extracted from the datacube and stored in a standard CSV format, as they allow each instance to be accurately mapped back to its corresponding original spatial location within the datacube.

The third auxiliary feature, `is_spain`, identifies the cells corresponding to Spanish territory, which are the only ones for which predictions should be generated. This layer was derived from a vectorial dataset containing the boundaries of Spain obtained from `simplemaps` [21] and processed with the QGIS software.

Given that these auxiliary features do not vary over time, they were stored as spatial features, with only the x and y coordinate values.

2.3 Fire history: EFFIS

The historical fire data for Spain were obtained using the EFFIS data request format [4]. The raw data were retrieved in vectorial format and contained geometries representing the burned area of historical fire events, along with the corresponding start and end dates of each fire event. To integrate this information into the datacube, the intersection of the spatial grid cells with the fire geometries in QGIS was calculated, as illustrated in Figure 4. Subsequently, a binary layer in the datacube, named `is_fire`, was created. A value of 1 was assigned to cells that intersected with fire geometries and fell within the corresponding temporal interval defined by the fire’s start and end dates. Following the definition of fire danger from [7], the previous process was executed on fires (geometries retrieved from EFFIS) with a burned area greater than 5 ha. This is because fire danger can be viewed as the combined risk of a fire igniting and the risk of that fire growing large (>5 ha). Introducing small wildfires as fire instances (`is_fire = 1`) could lead to inconsistencies, as these small fires did not grow larger for certain reasons (for example, high humidity). Therefore, the fire risk for these small fires was low, even though a fire was present.

After that, the `is_near_fire` layer was added, which is a binary feature indicating whether a cell is within a 25×25 cell area centred on each `is_fire = 1` instance, as well as the 10 days preceding the event. This results in a $25 \times 25 \times 10$ -sized box prior to each fire cell. This feature is useful for analysing the spatial and temporal proximity of fire occurrences, enabling the investigation of both the geographic and temporal closeness of future fires in relation to past events.

Both of these features were added to the datacube as spatio-temporal features, hence, with all three x , y , and t dimensions.

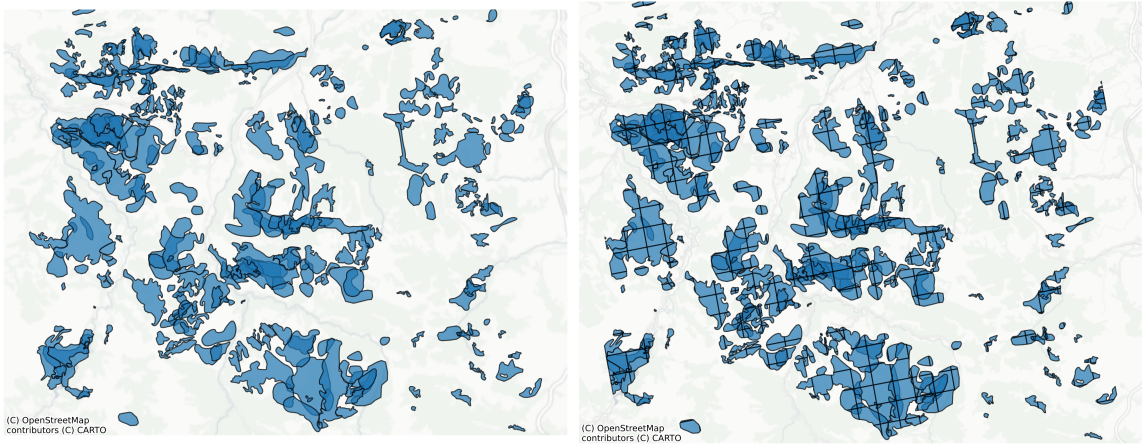


Figure 4: Left: raw geometries of the fire events downloaded from EFFIS. Right: the same geometries intersected with the spatial grid.

2.4 Geographical location information

The geographical location information included in the *IberFire* datacube plays a crucial role. As illustrated in Figure 1, certain regions inherently present a higher susceptibility to wildfires than others. Therefore, the inclusion of features representing the spatial position of each cell was deemed advantageous for the models.

Five features were added for this purpose: `x_coordinate`, `y_coordinate`, `is_sea`, `is_waterbody` and `AutonomousCommunities`. Since these geographical location features are time-invariant, they were stored in the datacube using only the spatial dimensions.

The first two features consist of the values of the coordinates of each cell in the EPSG:3035 coordinate reference system. The next two features, `is_sea` and `is_waterbody`, are binary indicators that denote whether a given cell is located over open sea or inland water, respectively. These features were calculated using QGIS with data from the European Digital Elevation Model.

Lastly, the `AutonomousCommunities` feature represents the level 2 NUTS (Nomenclature of Territorial Units for Statistics) [22] division of Spain, with values listed in Table 1. However, since the region of interest does not include Ceuta, Melilla, and the Canary Islands, the corresponding values for these regions do not appear in the dataset. The feature was generated in QGIS by converting a vector dataset containing the shapes of the autonomous communities of Spain [23] into a raster layer, assigning to each cell the corresponding value from Table 1 based on its intersection with the appropriate autonomous community.

Value	Region	Value	Region
0	Nodata	10	Comunidad Valenciana
1	Andalucía	11	Extremadura
2	Aragón	12	Galicia
3	Principado de Asturias	13	Comunidad de Madrid
4	Islas Baleares	14	Región de Murcia
5	Canarias	15	Comunidad Foral de Navarra
6	Cantabria	16	País Vasco
7	Castilla y León	17	La Rioja
8	Castilla - La Mancha	18	Ceuta
9	Cataluña	19	Melilla

Table 1: Values of the feature `AutonomousCommunities` and their corresponding regions.

All five geographic location information features remain invariant over time. Consequently, they were incorporated into the datacube only with spatial coordinates, without the time dimension.

2.5 Land usage: Corine Land Cover

The Copernicus Corine Land Cover (CLC) dataset [9] offers a standardized classification of land cover types across Europe, distinguishing 44 discrete categories. It represents the continent as a regular grid of 100m wide cells, assigning to each cell an integer value between 1 and 44 that corresponds to a specific land cover class.

As detailed in Table 2, each of the 44 land cover classes is associated with three hierarchical labels that facilitate their aggregation into broader thematic groups. The third label, Label 3, is the most specific, assigning a unique identifier to each of the 44 classes, therefore comprising 44 distinct categories. Label 2 serves as an intermediate level, grouping related Label 3 classes into broader categories, while Label 1 represents the highest level of aggregation, clustering the 44 land classes into 5 major land cover types.

Class	Label 1	Label 2	Label 3
1	Artificial surfaces	Urban fabric	Continuous urban fabric
2	Artificial surfaces	Urban fabric	Discontinuous urban fabric
3	Artificial surfaces	Industrial, commercial and transport units	Industrial or commercial units
4	Artificial surfaces	Industrial, commercial and transport units	Road and rail networks and associated land
5	Artificial surfaces	Industrial, commercial and transport units	Port areas
6	Artificial surfaces	Industrial, commercial and transport units	Airports
7	Artificial surfaces	Mine, dump and construction sites	Mineral extraction sites
8	Artificial surfaces	Mine, dump and construction sites	Dump sites
9	Artificial surfaces	Mine, dump and construction sites	Construction sites
10	Artificial surfaces	Artificial, non-agricultural vegetated areas	Green urban areas
11	Artificial surfaces	Artificial, non-agricultural vegetated areas	Sport and leisure facilities
12	Agricultural areas	Arable land	Non-irrigated arable land
13	Agricultural areas	Arable land	Permanently irrigated land
14	Agricultural areas	Arable land	Rice fields
15	Agricultural areas	Permanent crops	Vineyards
16	Agricultural areas	Permanent crops	Fruit trees and berry plantations
17	Agricultural areas	Permanent crops	Olive groves
18	Agricultural areas	Pastures	Pastures
19	Agricultural areas	Heterogeneous agricultural areas	Permanent crops ¹
20	Agricultural areas	Heterogeneous agricultural areas	Complex cultivation patterns
21	Agricultural areas	Heterogeneous agricultural areas	Land principally occupied by agriculture ¹
22	Agricultural areas	Heterogeneous agricultural areas	Agro-forestry areas
23	Forest and semi natural areas	Forests	Broad-leaved forest
24	Forest and semi natural areas	Forests	Coniferous forest
25	Forest and semi natural areas	Forests	Mixed forest
26	Forest and semi natural areas	Scrub and/or herbaceous vegetation associations	Natural grasslands
27	Forest and semi natural areas	Scrub and/or herbaceous vegetation associations	Moors and heathland
28	Forest and semi natural areas	Scrub and/or herbaceous vegetation associations	Sclerophyllous vegetation
29	Forest and semi natural areas	Scrub and/or herbaceous vegetation associations	Transitional woodland-shrub
30	Forest and semi natural areas	Open spaces with little or no vegetation	Beaches, dunes, sands
31	Forest and semi natural areas	Open spaces with little or no vegetation	Bare rocks
32	Forest and semi natural areas	Open spaces with little or no vegetation	Sparsely vegetated areas
33	Forest and semi natural areas	Open spaces with little or no vegetation	Burnt areas
34	Forest and semi natural areas	Open spaces with little or no vegetation	Glaciers and perpetual snow
35	Wetlands	Inland wetlands	Inland marshes
36	Wetlands	Inland wetlands	Peat bogs
37	Wetlands	Maritime wetlands	Salt marshes
38	Wetlands	Maritime wetlands	Salines
39	Wetlands	Maritime wetlands	Intertidal flats
40	Water bodies	Inland waters	Water courses
41	Water bodies	Inland waters	Water bodies
42	Water bodies	Marine waters	Coastal lagoons
43	Water bodies	Marine waters	Estuaries
44	Water bodies	Marine waters	Sea and ocean

Table 2: Definitions of the 44 classes from Corine Land Cover.

For instance, the class labelled as *Continuous urban fabric* in Label 3 is grouped under the category *Urban fabric* in Label 2, which, in turn, falls under the broader category *Artificial surfaces* in Label 1. More specifically, the category *Urban fabric* includes classes 1 and 2, whereas *Artificial surfaces* includes classes 1 through 11. This hierarchical structure enables both detailed analysis and higher-level generalization.

The original spatial resolution of the CLC dataset is 100m \times 100m; consequently, resampling of the data was needed to match the 1km \times 1km resolution of the *IberFire* datacube. Using QGIS, the proportion of each of the 44 classes within each 1km \times 1km cell was calculated. This resulted in 44 continuous features, denoted as CLC_1 for $i = 1, 2, \dots, 44$, with values ranging between 0 and 1.

Given that these features represent proportions and sum to 1 for each 1km \times 1km cell, and considering the hierarchical structure of the CLC classification, five additional features were derived corresponding to the higher-level groupings defined in Label 1. Specifically, for each higher-level category, its proportion within a cell was computed by summing the relevant CLC_1 variables that fall inside the category. For example, the proportion of *Artificial surfaces* was obtained by aggregating the values of CLC_1 through CLC_11.

The same procedure was applied to the intermediate level of the hierarchy, Label 2, resulting in the creation of 14 additional aggregated features. Although 15 categories exist at this level, the *Pastures* category (corresponding to class 18 in Label 3) was excluded, as it consists of a single class and thus provides no added abstraction over the original variable.

To recapitulate, a total of 63 explanatory variables were derived from the CLC dataset and incorporated into *IberFire*: 44 corresponding to the most detailed classification level Label 3, 14 to

¹Complete description shortened.

the intermediate level Label 2, and 5 to the highest level of aggregation Label 1.

The CLC dataset is updated every six years; accordingly, the 2006, 2012, and 2018 editions were used in this work, as the 2024 version was not yet available at the time of writing. As previously discussed, time-invariant features in the datacube can be stored using only spatial dimensions. Given the low update frequency of the CLC dataset, including a temporal dimension would result in unnecessary duplication of values. Therefore, all CLC-derived features were stored without the time axis. To differentiate between editions, the corresponding year was appended to each feature name, as better described in Table 6 of Section 3. Each of the three CLC editions contributed 63 variables, this approach ultimately yielded $63 \cdot 3 = 189$ distinct CLC-derived spatial features in the datacube.

2.6 Topography variables: European Digital Elevation Model

Topography is a well-established factor influencing the spread and intensity of forest fires. To capture these effects, topographic features were downloaded from the European Digital Elevation Model (EU-DEM) provided by OpenTopography [15]. The original EU-DEM dataset offers elevation values at a $30\text{m} \times 30\text{m}$ spatial resolution. Using this elevation data, additional variables such as slope, aspect and roughness of the terrain can be derived, all of which are also offered by OpenTopography.

However, the specific methods used by OpenTopography to calculate the slope and roughness are not documented, leaving the units of these variables undefined. In contrast, the aspect is expressed in degrees, ranging from 0° to 360° , indicating the direction in which the slope of each $30\text{m} \times 30\text{m}$ terrain cell faces, with 0° corresponding to the north and the values increasing clockwise.

The elevation, slope, roughness and aspect were downloaded and, for the first three features, the mean and standard deviation in each $1\text{km} \times 1\text{km}$ cell were calculated. Therefore, a total of 6 different features were obtained from elevation, slope, and roughness. For aspect, the feature was discretised into 8 different classes defined in Table 3. For each of the $1\text{km} \times 1\text{km}$ cell, the proportion of each class inside the cell was calculated, resulting in 8 new features called `aspect_i` for $i = 1, \dots, 8$. Additionally, an extra feature, `aspect_NODATA`, was included to represent the proportion of pixels within each $1\text{km} \times 1\text{km}$ cell for which no aspect value was available, which is highly correlated with `is_waterbody`. This lack of data typically occurs in areas covered by lakes and rivers, where aspect values are undefined due to the absence of terrain elevation gradients.

Class 1	Class 2	Class 3	Class 4	Class 5	Class 6	Class 7	Class 8
(0, 45]	(45, 90]	(90, 135]	(135, 180]	(180, 225]	(225, 270]	(270, 315]	(315, 360]

Table 3: Orientation classes grouped into 45° intervals.

These processes were performed using QGIS software, and the resulting 15 features were subsequently integrated into the datacube, utilizing only spatial coordinates.

2.7 Human activity

It is widely recognised that most wildfires are directly related to human activities, either intentionally or accidentally [24]. To model this phenomenon, six human-related explanatory variables were considered: distance to roads, distance to waterways, distance to railways, designation within the Natura 2000 protected network, population density, and holiday periods. These variables were used to derive a total of 20 features, which were subsequently integrated into the datacube.

The first two variables, distance to roads and distance to waterways, were obtained from WorldPop [16], which provides data at an approximate spatial resolution of $100\text{m} \times 100\text{m}$, represented in kilometres. To upscale the data to the target resolution, the mean and standard deviation within each $1\text{km} \times 1\text{km}$ cell were computed using QGIS. These aggregated statistics were then incorporated into the datacube, resulting in four derived features from the original two variables. These features were considered invariant over time and therefore added with only spatial coordinates.

For distance to railways, railway vectorial data in Spain were retrieved from OpenStreetMap [17]. Using QGIS, a $100\text{m} \times 100\text{m}$ raster layer was generated to represent the distance to the nearest railway geometry from each $100\text{m} \times 100\text{m}$ cell. Then, the same procedure was applied, and the average and standard deviation were calculated. These two features were then added to the datacube as spatial data.

The Natura 2000 network, a European ecological network for biodiversity conservation, was included due to its relevance in fire data reported by EFFIS, which indicates the proportion of fire

within these protected areas. Using vectorial boundaries of the Natura 2000 network [25], a binary raster layer was created with QGIS indicating whether each $1\text{km} \times 1\text{km}$ cell falls within the protected area. Since this variable remains constant over time, it was integrated as a spatial layer into the datacube.

Population density was incorporated as a proxy for human presence and potential ignition sources. Annual data were obtained from WorldPop for the years 2008 to 2020 [16], due to the unavailability of more recent data. The original data were retrieved with a resolution of approximately $1\text{km} \times 1\text{km}$, and average resampling was applied to match the coordinate values of *IberFire*. Given the annual update frequency of the data, population density were stored as spatial features to prevent unnecessary duplication of values, mirroring the process conducted with the CLC-derived features. As a result, this variable contributed 13 distinct spatial layers to the final dataset.

Finally, a binary feature representing holiday periods was included. This variable accounts for the increased presence of people in rural and natural areas during weekends and public holidays, potentially raising the risk of fire ignition. A cell was flagged as a holiday if the corresponding date was a Saturday, Sunday, or a national or regional public holiday in Spain. To determine public holidays, the Python library `holidays` [26] was utilized. This library provides holiday dates for various countries and their subdivisions, allowing for precise identification of holidays at the autonomous community level in Spain. Consequently, the `AutonomousCommunities` feature was employed to assign the appropriate regional holidays to each cell. The resulting `is_holiday` binary layer was added as a spatio-temporal feature within the datacube.

2.8 Meteorological variables: ERA5-Land

Meteorological conditions are among the most influential factors driving both the ignition and propagation of forest fires. Variables such as temperature, precipitation, and wind speed significantly affect fire behaviour and overall risk levels. Therefore, incorporating meteorological data into the datacube is essential for generating robust predictive models.

To account for these dynamics, data from ERA5-Land [10] were integrated, a high-resolution global reanalysis dataset provided by the Copernicus Climate Data Store. ERA5-Land offers hourly meteorological variables at a spatial resolution of $9\text{ km} \times 9\text{ km}$, from 1950 to the present. This dataset is particularly well-suited for environmental modelling due to its global coverage, temporal consistency, and availability of multiple curated atmospheric variables relevant to fire risk assessment. Within the Copernicus Climate Data Store, two data access modes are available: raw hourly observations and post-processed daily statistics. Both sources were used in the construction of the *IberFire* datacube, depending on the specific requirements of each variable.

Although ERA5-Land provides temporally consistent data, its availability is subject to a delay of five days, making it unsuitable for real-time fire risk prediction, where daily forecasts are required. Consequently, while ERA5-Land data were used to construct the datacube, real-time model deployment is intended to rely on meteorological station measurements. The use of measurements for the construction of the datacube was also considered, but the lack of historical data for many variables in various meteorological stations posed significant limitations.

AEMET (the Spanish Meteorological Agency) provides open-access, near real-time data from weather stations across Spain. Therefore, to ensure compatibility, all meteorological ERA5-Land features included in *IberFire* were selected and processed to align with the type and format of data provided by AEMET.

A total of 17 meteorological features were derived from ERA5-Land data. The features can be grouped as follows: temperature, relative humidity, surface pressure, precipitations, wind speed, and wind direction. This section outlines the methodology used to obtain and incorporate these variables into the *IberFire* datacube, including the selection of source variables and the transformations necessary to ensure compatibility with the format and units used in AEMET observations.

ERA5-Land data are available at a global scale; therefore, all relevant variables were extracted for the specific region of interest illustrated in Figure 1. To ensure spatial consistency across the entire datacube, all ERA5-Land data, originally provided at a resolution of $9\text{km} \times 9\text{km}$, were resampled to the target $1\text{ km} \times 1\text{ km}$ resolution using nearest-neighbour interpolation. All the meteorological features were added to the datacube as spatio-temporal variables, and the processing of these features was done using Python.

Temperature

Temperature plays a central role in wildfire risk modelling, as it directly affects the dryness and flammability of vegetation. Four daily statistics were saved to describe the temperature: mean, minimum, maximum, and range. The first three features were extracted from the daily statistics of the variable 2m temperature provided by ERA5-Land, which measures the temperature of the air at 2 metres above the surface of land. Then, the range, which is the difference between the daily maximum and minimum value, was calculated. Finally, the original units in Kelvin provided by ERA5-Land were transformed into Celsius, ensuring consistency with the units used by AEMET.

Relative humidity

Relative humidity is a critical variable for fire risk assessment, as it directly affects the moisture content of vegetation and, consequently, the likelihood of ignition and propagation. However, ERA5-Land does not provide this variable directly, while AEMET does. To address this, hourly relative humidity values were derived from two available ERA5-Land variables: the 2m temperature and the 2m dewpoint temperature. The last one represents the temperature at which the air becomes saturated with moisture, at 2 metres above the ground. Using these two temperature variables, relative humidity values were computed by applying the Magnus formula [27], an empirically validated approach for estimating saturation vapor pressure:

$$\text{Relative Humidity} = \frac{\exp\left(\frac{17.625 \cdot D_p}{243.04 + D_p}\right)}{\exp\left(\frac{17.625 \cdot T}{243.04 + T}\right)} \quad (1)$$

where D_p and T represent the 2m dewpoint temperature and 2m temperature in Celsius, respectively.

From the computed hourly values, four daily statistics were derived and included in the datacube: the mean, minimum, maximum, and range of relative humidity. This process required downloading and processing the full hourly time series of both temperature-related variables. Notice that the relative humidity daily statistics could not be accurately calculated from the ERA5-Land temperature summary statistics. For example, the mean of relative humidity can not be calculated by introducing the mean of D_p and T on the equation (1). The same happens for the other statistics too.

Surface pressure

Surface pressure values were retrieved from ERA5-Land as daily aggregated statistics, namely the mean, minimum, and maximum, originally expressed in pascals. Again, the daily range was then computed as the difference between the maximum and minimum values. Finally, all four features were converted to hectopascals to ensure consistency with the unit conventions used by AEMET.

Precipitations

Since pre-aggregated precipitation statistics were not available, hourly precipitation values were downloaded from ERA5-Land. These values, originally expressed in metres (equivalent to 1000 l/m²), were averaged to obtain daily mean precipitation values. Subsequently, the units were converted from metres to millimetres to ensure consistency with AEMET.

Wind speed

Wind-related features required particularly careful processing. ERA5-Land provides wind data in terms of its eastward (u-wind) and northward (v-wind) components, therefore, two hourly features, u-wind and v-wind, can be retrieved from ERA5-Land. In contrast, AEMET reports wind information as maximum and average wind speeds, without disaggregating it into horizontal and vertical components.

To align the ERA5-Land data with the format used by AEMET, hourly u-wind and v-wind values were retrieved from ERA5-Land. Then, the wind speed magnitude at each hour was computed using the Euclidean norm, taking into account the orthogonality of the components:

$$\|\vec{u} + \vec{v}\| = \|\vec{u}\| + \|\vec{v}\|. \quad (2)$$

From these hourly magnitudes, the daily maximum and average wind speeds were calculated and incorporated into the datacube as spatio-temporal features, named `wind_speed_max` and `wind_speed_mean`. The data were stored with the original ERA5-Land units, meters per second (m/s), since they match with the units used by AEMET.

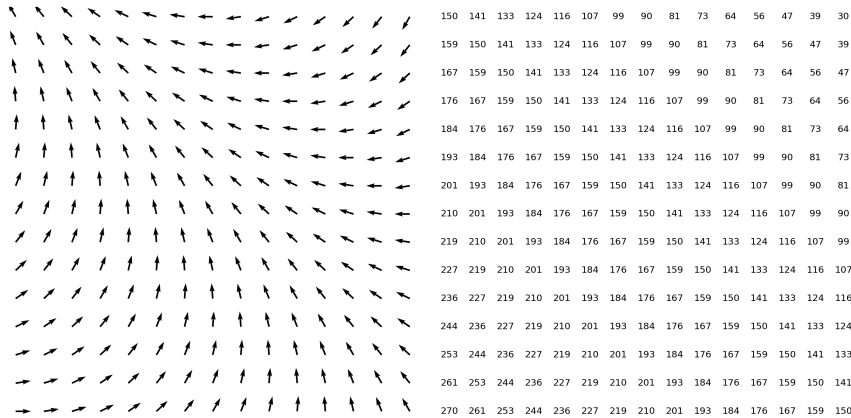


Figure 5: Left: wind vectors that represent the sum of ERA5-Land u-wind and v-wind components. Right: the wind direction values of those same vectors.

It is important to note that, analogous to the case of relative humidity, daily wind speed statistics cannot be accurately computed from the daily maximum or average values of u-wind and v-wind individually. The magnitude must be calculated at the hourly level before aggregation.

Wind direction

Wind direction is conventionally defined as the direction from which the wind originates, expressed in degrees measured clockwise from true north. AEMET provides two daily wind-direction metrics: the average wind direction and the direction at the daily maximum wind speed. Meanwhile, ERA5-Land offers hourly wind data at a resolution of $9\text{km} \times 9\text{km}$, represented by horizontal (u_wind) and vertical (v_wind) components. To convert these components into standard wind direction, equation (3) is employed, where α denotes the angle between (u, v) and the north vector $(0, 1)$.

$$\text{Wind direction} = (\alpha - 180^\circ) \bmod 360^\circ, \quad \alpha = \angle((0, 1), (u, v)). \quad (3)$$

Figure 5 demonstrates this process by comparing the original component-wise data from ERA5-Land on the left, with the derived wind direction map on the right.

To obtain the daily average wind direction, daily averaged values of u_wind and v_wind were first obtained from ERA5-Land’s aggregated statistics and converted with equation 3. Subsequently, to capture the direction at each day’s maximum wind speed, hourly u_wind and v_wind components were downloaded, and equation (3) was applied at each hourly timestamp. The direction corresponding to the highest wind speed of the day was then retained. This resulted in the addition of two spatio-temporal features, `wind_direction.mean` and `wind_direction.at_max_speed`.

2.9 Vegetation indices: Copernicus Land Monitoring Service

The last group of features integrated into the datacube is the vegetation indices, which are highly used for making fire-risk predictions, as they can represent the dryness of the plant life. Five different indices were added: *FAPAR* (Fraction of Photosynthetically Active Radiation), *LAI* (Leaf Area Index), *NDVI* (Normalized Difference Water Index), *LST* (Land Surface Index), and *SWI* (Soil Water Index). All of them were retrieved from the Copernicus Land Monitoring Service (CLMS) [11] at various spatial and temporal resolutions.

For each vegetation index, multiple data sources from the Copernicus Land Monitoring Service (CLMS) were employed, each differing in spatial and temporal resolution. Depending on the source, some datasets provide global coverage, while others are limited to the European continent. To ensure efficiency and relevance, the data were downloaded specifically for the region of interest illustrated in Figure 1. The following sections offer a detailed description of the sources selected for each index, the procedures followed during data acquisition, and the preprocessing steps applied to harmonise all variables with the target spatial resolution of $1\text{km} \times 1\text{km}$ and daily temporal granularity required by the *IberFire* datacube. This process was done using Python, and all the vegetation indices were incorporated into the dataset as spatio-temporal features.

FAPAR

The Fraction of Absorbed Photosynthetically Active Radiation (FAPAR) is a key biophysical variable that is commonly used as an indicator of vegetation health. It has been identified as one of the 50 Essential Climate Variables (ECVs) by the Global Climate Observing System (GCOS) [28]. In the context of wildfire risk prediction, FAPAR is particularly relevant as it reflects the photosynthetic activity and water stress level of vegetation, which are tightly linked to fuel dryness.

The CLMS provides multiple datasets for the FAPAR variable; however, no single source spans the entire temporal range required by the *IberFire* datacube. To achieve full temporal coverage, two complementary datasets were integrated. The first source offers FAPAR measurements at a spatial resolution of $1\text{km} \times 1\text{km}$ with a 10-day temporal frequency and was used to cover the period from 01/12/2007 to 30/04/2020. The second source, used for the remaining period from 01/05/2020 to 31/12/2024, provides enhanced spatial resolution at $300\text{m} \times 300\text{m}$, while maintaining the same temporal frequency.

The two datasets were harmonized as follows. For the first source, since its native resolution matched the target resolution of the datacube, values were directly aligned to the grid using nearest-neighbour resampling. In contrast, the higher-resolution values from the second source were aggregated by computing the mean FAPAR value within each corresponding $1\text{km} \times 1\text{km}$ cell, effectively applying the average resampling method.

LAI

The Leaf Area Index (LAI) represents the total one-sided green leaf area per unit ground area (m^2/m^2) and is a key indicator of vegetation density and structure. It is also one of the Essential Climate Variables (ECVs) identified by the GCOS, and is widely used in ecological modelling and fire risk assessment.

The download and preprocessing procedures for this variable followed the same approach as for the FAPAR index. A dataset with a 1 km spatial resolution was used for the period from 01/12/2007 to 30/04/2020 and was aligned to the datacube using nearest-neighbour resampling. For the remaining period, from 01/05/2020 to 31/12/2024, a dataset at 300 m resolution was employed, and values were aggregated to 1 km resolution using average resampling.

NDVI

The Normalized Difference Vegetation Index (NDVI) is a remote sensing indicator that estimates vegetation health. It is calculated from the red and near-infrared spectral bands and typically ranges from -1 to 1 , with higher values indicating denser and healthier vegetation. In the context of wildfire risk assessment, NDVI serves as a proxy for vegetation condition and fuel availability.

As with the previous indices, two complementary datasets from the CLMS were used to ensure full temporal coverage. The first dataset, with a spatial resolution of $1\text{km} \times 1\text{km}$ and a 10-day frequency, covers the period from 01/12/2007 to 30/06/2020. The second dataset, with a finer resolution of 300 m and the same temporal frequency, was used from 01/07/2020 to 31/12/2024. The harmonization process mirrored that used for FAPAR and LAI: nearest-neighbour resampling was applied to the 1 km dataset, while the 300 m data were aggregated to 1 km using average resampling.

LST

The Land Surface Temperature (LST) represents the skin temperature of the land, expressed in Kelvin. Unlike other vegetation indices, *LST* is available in CLMS as an hourly variable. However, due to limitations in the temporal extents of individual datasets, three complementary sources were used to ensure full temporal coverage of the *IberFire* datacube.

For the period from 01/12/2007 to 10/06/2010, LST values were obtained from the aggregated ERA5-Land dataset, which provides global daily average skin temperature estimates at a spatial resolution of $9\text{km} \times 9\text{km}$. From 11/06/2010 to 18/01/2021, a CLMS source offering hourly LST at a resolution of $5\text{km} \times 5\text{km}$ was used. For each timestamp, the daily average value was calculated from retrieved hourly values. Finally, from 19/01/2021 to 31/12/2024, a second CLMS source was used, also with hourly values with $5\text{km} \times 5\text{km}$ resolution, and the same daily temporal averaging method was applied.

Finally, to harmonise all three datasets with the $1\text{km} \times 1\text{km}$ resolution of *IberFire*, nearest-neighbour resampling was applied in each case.

SWI

The Soil Water Index (SWI) is a moisture-related indicator that estimates the percentage of water retained in the upper layers of the soil. It is derived from observations of Surface Soil Moisture (SSM) using an exponential filtering approach, giving more weight to recent measurements while smoothing the temporal signal [29].

Equation 4 calculates SWI for time t_n based on past SSM measurements on times t_i with $i < n$:

$$SWI(t_n) = \frac{\sum_i^n SSM(t_i) e^{-\frac{t_n-t_i}{T}}}{\sum_i^n e^{-\frac{t_n-t_i}{T}}}. \quad (4)$$

The parameter T regulates the influence of past observations, with smaller T values assigning greater weight to recent measurements and larger T values producing a more temporally smoothed index. For instance, with $T = 1$, a measurement taken 10 days prior contributes with a weight proportional to $e^{-\frac{10}{1}} \approx 4.5 \cdot 10^{-5}$, whereas with $T = 10$ the same observation has a weight proportional to $e^{-\frac{10}{10}} \approx 0.37$.

To capture moisture dynamics at different temporal scales, four SWI variants were downloaded and included in the datacube, corresponding to $T = 1, 5, 10, 20$ and named *SWI_001*, *SWI_005*, *SWI_010*, *SWI_020* respectively. The data were retrieved from CLMS, which provides daily SWI values at a spatial resolution of $12.5\text{km} \times 12.5\text{km}$. To align with the datacube's $1\text{ km} \times 1\text{ km}$ resolution, nearest-neighbour interpolation was applied during the resampling process.

2.10 Summary of external data sources

To ensure transparency and reproducibility, Table 4 provides direct links to the original raw datasets used in the construction of the *IberFire* datacube. These sources include official and publicly accessible repositories from European and national institutions. Each dataset listed in the table corresponds to one or more features included in the datacube, and their inclusion allows users to verify data provenance, explore updates, or perform additional processing tailored to specific needs.

Category	Retrieved feature	Resolution	Original Source
Auxiliary features	Spain boundary	Geometries	https://simplemaps.com/gis/country/es
Fire history	Historical fire data	Geometries	https://forest-fire.emergency.copernicus.eu/apps/data.request.form/
Geographical location	Autonomous Communities	Geometries	https://www.arcgis.com/home/item.html?id=5f689357238847bc823a2fb164544a77
Land usage	CLC_2006, CLC_2012, CLC_2018	100m	https://land.copernicus.eu/en/products/corine-land-cover/
Topography	Elevation, slope, aspect, roughness	30m	https://portal.opentopography.org/raster?opentopoID=OTSDEM.032021.4326.3
Human activity	Population density	1km	https://hub.worldpop.org/geodata/listing?id=76
	Distance to roads	100m	https://hub.worldpop.org/geodata/summary?id=17504
	Distance to waterways	100m	https://hub.worldpop.org/geodata/summary?id=18002
	Railways raw data	Geometries	https://download.geofabrik.de/europe/spain.html
Meteorological	Natura 2000 network	Geometries	https://www.miteco.gob.es/es/biodiversidad/servicios/banco-datos-naturaleza/informacion-disponible/rednatura_2000_desc.html
	2m temperature, surface pressure, 10m u-wind, 10m v-wind	9km, hourly	https://cds.climate.copernicus.eu/datasets/reanalysis-era5-land
Vegetation	FAPAR	1km, 10-daily	https://land.copernicus.eu/en/products/vegetation/fraction-of-absorbed-photosynthetically-active-radiation-v2-0-1km
		300m, 10-daily	https://land.copernicus.eu/en/products/vegetation/fraction-of-absorbed-photosynthetically-active-radiation-v1-0-300m
	LAI	1km, 10-daily	https://land.copernicus.eu/en/products/vegetation/leaf-area-index-v2-0-1km
		300m, 10-daily	https://land.copernicus.eu/en/products/vegetation/leaf-area-index-300m-v1.0
	NDVI	1km, 10-daily	https://land.copernicus.eu/en/products/vegetation/normalised-difference-vegetation-index-v3-0-1km
		300m, 10-daily	https://land.copernicus.eu/en/products/vegetation/normalised-difference-vegetation-index-v2-0-300m
LST	9km, daily	https://cds.climate.copernicus.eu/datasets/derived-era5-land-daily-statistics?tab=overview	
	5km, hourly	https://land.copernicus.eu/en/products/temperature-and-reflectance/hourly-land-surface-temperature-global-v1-0-5km	
	5km, hourly	https://land.copernicus.eu/en/products/temperature-and-reflectance/hourly-land-surface-temperature-global-v2-0-5km	
SWI_01, SWI_05, SWI_10, SWI_20	12.5km, daily	https://land.copernicus.eu/en/products/soil-moisture/daily-soil-water-index-global-v3-0-12-5km	

Table 4: Links to the sources of the raw data used in the construction of the *IberFire* datacube.

3 Data Records

The *IberFire* datacube comprises approximately $6.8 \cdot 10^9$ individual cells, resulting from the combination of 1188 values along the x coordinate, 920 along the y coordinate, and 6241 distinct timestamps. Each (x, y, t) cell stores a vector of 260 features that include static and dynamic variables relevant to wildfire risk modelling. At any given cell, all 260 feature values can be retrieved for analytical or predictive purposes. This chapter presents a detailed description of the 260 features, organised into structured tables that replicate the format found on *IberFire* when opened with `xarray`.

The datacube is publicly available on Zenodo (<https://zenodo.org/records/15225886>), and the variables are organised in the following tables according to the categories defined in Chapter 2. Table 5 presents the three auxiliary features, two fire-related variables, and five geographic context features. Table 6 details the 63 variables derived from the 2006 Corine Land Cover dataset. Table 7 then presents the 15 topographical and 21 human activity features. Lastly, Table 8 summarises the 17 meteorological variables and 8 vegetation indices included in the dataset. *IberFire* contains 126 additional features derived from the 2012 and 2018 CLC datasets. As those features follow the same structure as the 2006 version, they are not described separately.

Feature Name	Description	Values or Units
x_index	X-coordinate index values	Integer in [0, 1187]
y_index	Y-coordinate index values	Integer in [0, 919]
is_spain	Binary mask indicating the Spanish region	0 (outside Spain), 1 (inside Spain)
is_fire	Binary indicator denoting whether the cell was affected by a fire on that date.	0 (no fire), 1 (fire)
is_near_fire	Binary indicator showing if the cell is within a 25×25 spatial area and a 10-day window preceding a fire event.	0 (not near fire), 1 (near fire)
x_coordinate	X-coordinate values in the EPSG:3035 reference system	Meters
y_coordinate	Y-coordinate values in the EPSG:3035 reference system	Meters
is_sea	Binary indicator denoting whether a cell lies over the open sea. The data was derived from the Copernicus Global Digital Elevation Model	0 (land), 1 (sea)
is_waterbody	Binary indicator denoting whether a cell lies over inland water (e.g., lakes, rivers). The data was derived from the Copernicus Global Digital Elevation Model	0 (non-water), 1 (inland water)
AutonomusCommunity	The Autonomous Communities code	Label from 00 to 19

Table 5: Top table: auxiliary features. Middle table: fire history features. Bottom table: geographical location features.

Feature Name	Description
CLC_2006_1 (...) CLC_2006_44	Proportion of original grid cells labelled as class 1 in CLC in the $1km \times 1km$ cell Proportion of original grid cells labelled as class 44 in CLC in the $1km \times 1km$ cell
CLC_2006_urban_fabric_proportion CLC_2006_industrial_proportion CLC_2006_mine_proportion CLC_2006_artificial _vegetation_proportion CLC_2006_arable_land_proportion CLC_2006_permanent_crops_proportion CLC_2006_heterogeneous _agricultural_proportion CLC_2006_forest_proportion CLC_2006_scrub_proportion CLC_2006_open_space_proportion	Proportion of original cells labelled as class 1 or 2 in CLC in the $1km \times 1km$ cell Proportion of original cells labelled as class 3, 4, 5 or 6 in CLC in the $1km \times 1km$ cell Proportion of original cells labelled as class 7, 8 or 9 in CLC in the $1km \times 1km$ cell Proportion of original cells labelled as class 10 or 11 in CLC in the $1km \times 1km$ cell Proportion of original cells labelled as class 12, 13 or 14 in CLC in the $1km \times 1km$ cell Proportion of original cells labelled as class 15, 16 or 17 in CLC in the $1km \times 1km$ cell Proportion of original cells labelled as class 19, 20 or 21 in CLC in the $1km \times 1km$ cell
CLC_2006_inland_wetlands_proportion CLC_2006_maritime_wetlands_proportion CLC_2006_inland_waters_proportion CLC_2006_marine_waters_proportion	Proportion of original cells labelled as class 23, 24 or 25 in CLC in the $1km \times 1km$ cell Proportion of original cells labelled as class 26, 27, 28 or 29 in CLC in the $1km \times 1km$ cell Proportion of original cells labelled as class 30, 31, 32, 33 or 34 in CLC in the $1km \times 1km$ cell Proportion of original cells labelled as class 35 or 36 in CLC in the $1km \times 1km$ cell Proportion of original cells labelled as class 37, 38 or 39 in CLC in the $1km \times 1km$ cell Proportion of original cells labelled as class 40 or 41 in CLC in the $1km \times 1km$ cell Proportion of original cells labelled as class 42, 43 or 44 in CLC in the $1km \times 1km$ cell
CLC_2006_artificial_proportion CLC_2006_agricultural_proportion CLC_2006_forest_and_semi _natural_proportion CLC_2006_wetlands_proportion CLC_2006_waterbody_proportion	Proportion of original cells labelled as classes from 1 to 11 in CLC in the $1km \times 1km$ cell Proportion of original cells labelled as classes from 12 to 22 in CLC in the $1km \times 1km$ cell Proportion of original cells labelled as classes from 23 to 34 in CLC in the $1km \times 1km$ cell Proportion of original cells labelled as classes from 35 to 39 in CLC in the $1km \times 1km$ cell Proportion of original cells labelled as classes from 40 to 44 in CLC in the $1km \times 1km$ cell

Table 6: Corine Land Cover features (corresponding to 2006). All features correspond to proportions, with values ranging from 0 to 1. The top part describes the 44 raw classes of the CLC dataset. The middle part corresponds to the 14 intermediate aggregation levels. The lower part of the table represents the 5 higher clustering levels of CLC. This hierarchical ordering is defined in Table 2.

Feature Name	Description	Values or Units
elevation_mean	Mean elevation in the 1 km × 1 km grid cell. The elevation is computed from the Digital Elevation Model (DEM) at 30 m resolution	Meters
elevation_stdev	Standard deviation in the 1 km × 1 km grid cell. The elevation is computed from the Digital Elevation Model (DEM) at 30 m resolution	Meters
slope_mean	Mean slope in the 1 km × 1 km grid cell. The slope is computed from the Digital Elevation Model (DEM) at 30 m resolution	-
slope_stdev	Standard deviation slope in the 1 km × 1 km grid cell. The slope is computed from the Digital Elevation Model (DEM) at 30 m resolution	-
roughness_mean	Mean roughness in the 1 km × 1 km grid cell. The roughness is computed from the Digital Elevation Model (DEM) at 30 m resolution	-
roughness_stdev	Standard deviation roughness in the 1 km × 1 km grid cell. The roughness is computed from the Digital Elevation Model (DEM) at 30 m resolution	-
aspect_1	Proportion of the aspect class 1 in the 1 km × 1 km grid cell. The aspect classes are computed from the digital elevation model (DEM) and represent the orientation of the terrain	Proportion [0,1]
(...)		
aspect_8	Proportion of the aspect class 8 in the 1 km × 1 km grid cell. The aspect classes are computed from the digital elevation model (DEM) and represent the orientation of the terrain	Proportion [0,1]
aspect_NODATA	Proportion of the aspect class NODATA in the 1 km × 1 km grid cell. The aspect classes are computed from the digital elevation model (DEM) and represent the orientation of the terrain	Proportion [0,1]
dist_to_roads_mean	Mean distance to roads in the 1 km × 1 km grid cell	Kilometers
dist_to_roads_stdev	Standard deviation of the distance to roads in the 1 km × 1 km grid cell	Kilometers
dist_to_waterways_mean	Mean distance to waterways in the 1 km × 1 km grid cell	Kilometers
dist_to_waterways_stdev	Standard deviation of the distance to waterways in the 1 km × 1 km grid cell	Kilometers
dist_to_railways_mean	Mean distance to railways in the 1 km × 1 km grid cell	-
dist_to_railways_stdev	Standard deviation of the distance to railways in the 1 km × 1 km grid cell	-
is_holiday	Binary mask indicating whether it is a holiday in the 1 km × 1 km grid cell in that time or not	0 (working day), 1 (holiday)
is_natura2000	Binary mask indicating whether the 1 km × 1 km grid cell is part of the Natura 2000 network or not	0 (is not in Natura 2000), 1 (is in Natura 2000)
popdens_2008	Mean population density in the 1 km × 1 km grid cell for the year 2008	People/ km^2
(...)		
popdens_2020	Mean population density in the 1 km × 1 km grid cell for the year 2020	People/ km^2

Table 7: Top: topography features. Bottom: human activity features.

Feature Name	Description	Values or Units
t2m_mean	The mean temperature of air measured at 2m above the surface of the land, sea or inland waters	Celsius
t2m_min	The minimum temperature of air measured at 2m above the surface of the land, sea or inland waters	Celsius
t2m_max	The maximum temperature of air measured at 2m above the surface of the land, sea or inland waters	Celsius
t2m_range	The range temperature of air measured at 2m above the surface of the land, sea or inland waters	Celsius
RH_mean	The mean relative humidity of air	[0, 100] in %
RH_min	The minimum relative humidity of air	[0, 100] in %
RH_max	The maximum relative humidity of air	[0, 100] in %
RH_range	The range relative humidity of air	[0, 100] in %
surface_pressure_mean	The mean surface pressure of air	Hectopascal
surface_pressure_min	The minimum surface pressure of air	Hectopascal
surface_pressure_max	The maximum surface pressure of air	Hectopascal
surface_pressure_range	The range surface pressure of air	Hectopascal
total_precipitation_mean	Mean of the hourly values of the total precipitation variable from ERA5-Land	millimetres (1l/m ²)
wind_speed_mean	The mean wind speed derived from the hourly u-component and v-component of wind	Meters per second (m/s)
wind_speed_max	The maximum wind speed derived from the hourly u-component and v-component of wind	Meters per second (m/s)
wind_direction_mean	The mean wind direction (where the wind comes) derived from the mean u-component and v-component of wind	Degrees
wind_direction_at_max_speed	The wind direction (where the wind comes) where the maximum wind speed happened. Derived after calculating the hourly wind speed from the hourly u-component and v-component of wind	Degrees
fapar	Fraction of Absorbed Photosynthetically Active Radiation, the fraction of the solar radiation absorbed by live plants for photosynthesis	-
lai	Leaf Area Index, representing the half of the total green canopy area per unit horizontal ground area	-
LST	Land Surface Temperature is the temperature of the surface of the Earth	Kelvin
ndvi	Normalized Difference Vegetation Index, an indicator of the greenness of the biomes	-
SWI_001	Soil Water Index at T=1, provides daily updates on the moisture conditions in different soil layers	[0, 100] in %
SWI_005	Soil Water Index at T=5, provides daily updates on the moisture conditions in different soil layers	[0, 100] in %
SWI_010	Soil Water Index at T=10, provides daily updates on the moisture conditions in different soil layers	[0, 100] in %
SWI_020	Soil Water Index at T=20, provides daily updates on the moisture conditions in different soil layers	[0, 100] in %

Table 8: Top: meteorological features. Bottom: vegetation indices.

4 Technical Validation

Four distinct validation procedures were conducted to ensure the robustness and reliability of *IberFire*. First, the integrity of data formats and measurement units was verified to guarantee internal consistency across all features. Second, given that vegetation indices were derived from satellite-based remote sensing data, the presence of missing values was common. To address this, multiple imputation techniques were evaluated, and the method yielding the lowest reconstruction error was applied to fill missing data. Third, available AEMET historical measurement data were downloaded and compared with *IberFire* meteorological data. Finally, an XGBoost model was trained on data from 2008 to 2023 and fire risk maps were plotted in various 2024 days, which served as a practical validation step to assess the predictive utility of *IberFire*. This chapter provides a detailed account of each of these four validation strategies aimed at guaranteeing the quality and usability of the *IberFire* datacube.

4.1 Data correctness

A datacube is a multi-dimensional data structure that integrates spatial and temporal information in a unified framework. Within the *IberFire* datacube, this includes coordinate grids, binary and categorical attributes, proportion-based data, and continuous numerical features. Given the complexity and heterogeneity of these components, quality assurance procedures are needed to ensure the reliability and internal consistency of the datacube. This section outlines the validation processes carried out to assess the correctness of temporal coordinates, the integrity of categorical and binary variables, the validity of proportion-based attributes, and the credibility of numerical values. These checks were designed to detect anomalies and confirm that the data adheres to defined structural standard across the entire temporal range of the datacube.

First, a temporal consistency check was conducted to guarantee that there are no duplicated time coordinates in the datacube. The dataset was verified to contain valid accessible values for all spatio-temporal features across the entire temporal range from 01/12/2007 to 31/12/2024. For the spatial features, visual inspection was performed to ensure that spatial coordinates are homogeneous across all the region of interest.

For categorical and binary features, it was ensured that all entries conformed to the expected set of values. For the `AutonomousCommunities` feature, all labels were verified to fall within the valid range of 0 to 19, with no occurrences of invalid or unexpected values. Regarding binary features, `is_spain`, `is_sea`, `is_waterbody`, `is_holiday`, `is_natura2000`, `is_fire`, and `is_near_fire`, it was confirmed that all values were strictly limited to either 0 or 1.

For features representing proportions, such as the nine derived from aspect and the 189 calculated from CLC, data validation procedures ensured that all values lie within the range $[0, 1]$, with no values falling outside this interval. Similarly, features derived from Relative Humidity and the four indices based on the Soil Water Index (SWI), which represent percentages, were verified to exclusively contain numerical values within the interval $[0, 100]$.

Additionally, for the proportion-based features derived from the CLC dataset, structured hierarchically into three levels as outlined in Section 2.5, consistency checks were performed to ensure that the proportions at each hierarchical level sum to one for every cell. Therefore, it was verified that the five aggregated features at Label 1, the fourteen intermediate-level features at Label 2, and the forty-four fine-grained features at Label 3 each sum to exactly one per cell.

Finally, for numerical features such as meteorological variables and vegetation indices, visual inspection was carried out through exploratory plotting to identify potential outliers and ensure that all values fell within logical and expected ranges. This process revealed a substantial number of missing values in certain data sources used to construct the vegetation indices. For instance, in the case of `FAPAR`, no missing values were observed until 30/04/2020, which corresponds to the ending of the first data source. After that date, the second source was used and exhibited a considerable number of gaps. The methodology adopted to address this issue is detailed in the following section.

4.2 Missing values validation

Once all features were validated to fall within their expected formats and value ranges, the missing values identified in the vegetation indices were subsequently addressed. To do so, different interpolation techniques were compared, and the one with the lowest reconstruction error was applied. This step was crucial, as not all machine learning algorithms can inherently manage missing data.

The imputation process was applied exclusively to the vegetation indices, as the remaining data sources were either complete or contained a negligible amount of missing values. In particular, no missing data were observed in any of the spatial-only features. Regarding spatio-temporal features, the layers `is_fire`, `is_near_fire`, and `is_holiday` were complete for the entire temporal range. Likewise, the meteorological variables derived from the ERA5-Land dataset did not exhibit missing values within the Spanish territory (`is_spain = 1`), due to the spatial continuity and post-processing of the source data.

To address the missing values in the vegetation indices, several imputation techniques were evaluated by introducing artificial gaps in dates known to be complete. The introduced gaps followed the real shapes of the missing values observed in satellite-derived vegetation indices. Subsequently, various imputation methods were applied to reconstruct the artificially masked values, and the reconstruction accuracy of each method was quantified using the Mean Absolute Error (MAE). This evaluation was performed independently for each vegetation index.

Four imputation techniques were selected for evaluation: nearest neighbour, linear, quadratic, and cubic interpolation. Each method was applied along the temporal axis, and linear interpolation yielded the lowest reconstruction errors across every tested feature. Consequently, it was adopted as the imputation method for filling missing values in the vegetation indices.

4.3 Data comparison with AEMET

The *IberFire* datacube was constructed to support daily-scale applications that use meteorological data from AEMET. Given that the meteorological variables were derived from ERA5-Land data and subsequently transformed to align with the format of AEMET observations, a validation process was carried out to evaluate the accuracy of these transformations.

This validation involved comparing the final, transformed ERA5-Land variables included in *IberFire* against historical records from AEMET meteorological stations. Particular attention was paid to the *u-wind* and *v-wind* components, which underwent the most complex transformations, as they required the reconstruction of wind speed and direction.

To perform the comparison, historical AEMET data were retrieved from <https://datosclima.es/Aemethistorico/Descargahistorico.html>. This source provides daily records from meteorological stations, including maximum, mean, and minimum temperature, precipitation, mean wind speed, wind direction at maximum wind speed, maximum wind speed, and both maximum and minimum surface pressure. Unfortunately, this source does not include historical records for other meteorological variables featured in *IberFire*, such as relative humidity. No alternative source was found that offers historical records for these variables. Furthermore, the retrieved AEMET dataset contained missing values for the available variables, and many of those features were not provided in all stations.

For each meteorological station within the region of interest, the Mean Absolute Error (MAE) was calculated for all available dates between 01/01/2007 and 31/12/2024, across all available features. Selected examples of these results are shown in the top four images of Figure 6. As illustrated, precipitation records are available for a considerably larger number of stations as opposed to those of surface pressure. Not only that, some stations have higher MAE values than others on the same feature.

Given the substantial regional variability in meteorological conditions, for example, the significantly higher precipitation levels in northern Spain compared to the south, a normalisation step was introduced to enable consistent comparisons of error magnitudes across features and stations. To this end, the Normalised Mean Absolute Error (NMAE) was computed according to the following expression:

$$\text{NMAE}(\text{feature}, \text{station}) = \frac{\text{MAE}(\text{feature}, \text{station})}{\max(\text{feature}, \text{station}) - \min(\text{feature}, \text{station})}, \quad (5)$$

where $\text{MAE}(\text{feature}, \text{station})$ is the MAE value of a feature in a given station, $\max(\text{feature}, \text{station})$ is the maximum value of the feature measured in that station, and $\min(\text{feature}, \text{station})$ is the minimum. Table 9 provides the mean MAE and NMAE values across all stations for every available feature, and the bottom two images of Figure 6 visually compare the NMAE values with violin and density plots.

The results indicate that the temperature features are highly reliable. Even in the worst-performing station, the mean Mean Absolute Error (MAE) remains as low as 2.173, with a standard deviation of 1.215. Assuming a normal distribution of errors, this implies that in 95% of the cases, the discrepancy between AEMET measurements and *IberFire* data does not exceed 4°. Given that

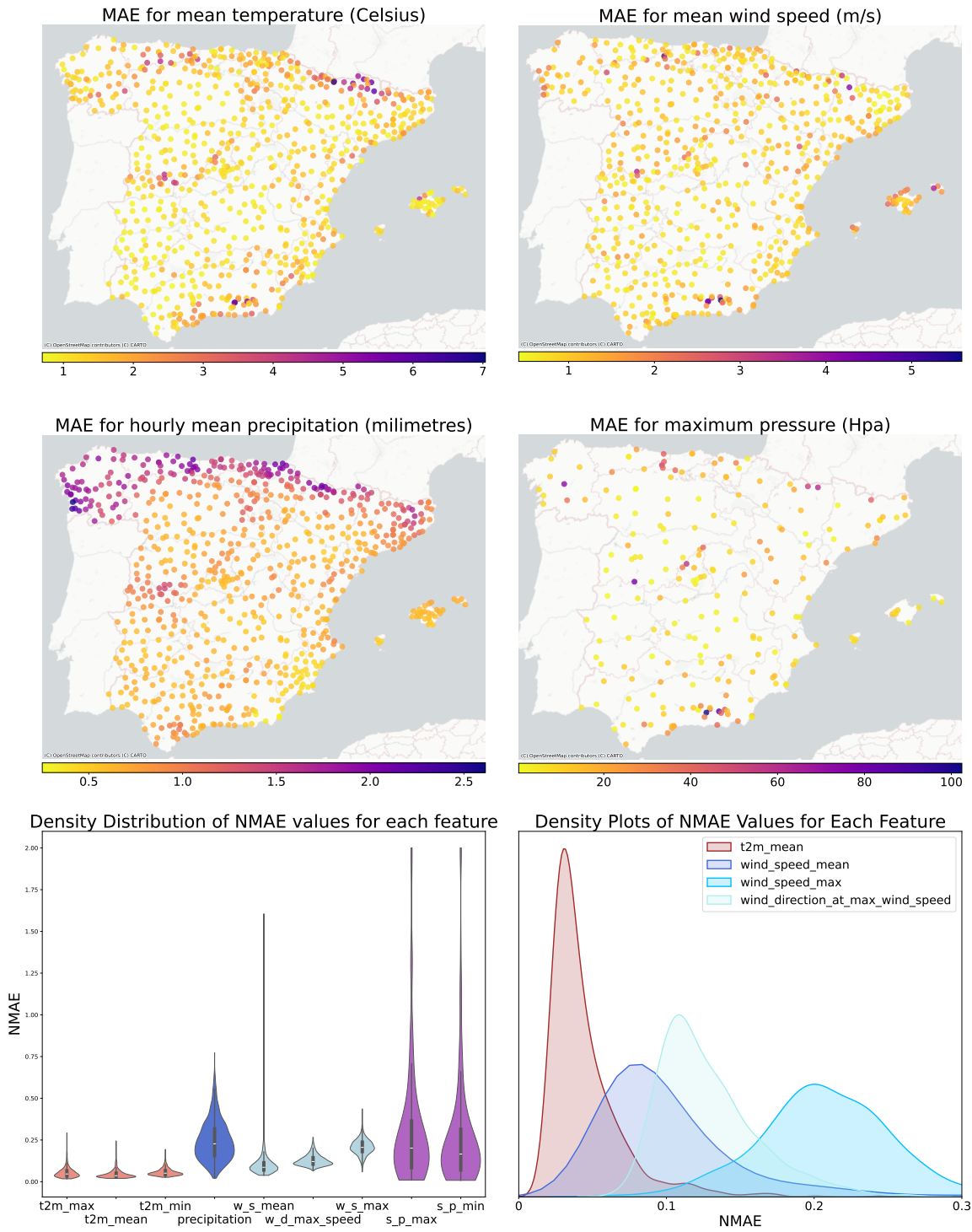


Figure 6: Four upper images: MAE values in the available stations for `t2m_mean`, `wind_speed_mean`, `total_precipitation_mean`, `surface_pressure_max`. Bottom left: violin plot with NMAE values for all variables. Bottom right: density plot with NMAE values for the features with the most distinct NMAE distributions.

	t2m_max	t2m_mean	t2m_min	precip.	w_s_mean	w_d_max_s	w_s_max	s_p_max	s_p_min
mean_MAE	2.173	1.495	1.829	0.918	1.046	46.115	5.856	13.995	13.738
stdev_MAE	1.215	0.815	0.732	0.422	0.563	11.841	1.728	15.546	15.531
mean_NMAE	0.055	0.045	0.058	0.246	0.104	0.128	0.209	0.356	0.312
stdev_NMAE	0.032	0.026	0.024	0.118	0.08	0.033	0.047	0.629	0.603
#NA_values	58	58	58	67	169	169	169	605	605

Table 9: Summary of MAE and NMAE metric values. Feature names from left to right: `t2m_max`, `t2m_mean`, `t2m_min`, `total_precipitation_mean`, `wind_speed_mean`, `wind_direction_at_max_speed`, `wind_speed_max`, `surface_pressure_max`, and `surface_pressure_min`.

temperature values at a single station can vary by up to 40° across different days, this error value is relatively small and supports the robustness of the temperature variables in the *IberFire* datacube. Moreover, as the temperature values are derived from ERA5-Land, a dataset rigorously validated by the Copernicus Climate Data Store, their reliability is further reinforced.

In comparison, the precipitation and surface pressure features exhibit higher NMAE values than temperature. Nevertheless, these variables are also sourced from Copernicus ERA5-Land, a dataset extensively validated. Consequently, despite their relatively higher error metrics, the integrity and reliability of these features remain supported by the quality and consistency of the underlying data source.

Finally, the wind-related features yield intermediate NMAE values. These variables underwent the most substantial transformations, involving the reconstruction of magnitudes and angles from vector components. Despite the complexity of the transformations, the resulting error values remain within acceptable bounds, suggesting that the transformation procedures were effective and that the wind features in the *IberFire* datacube are suitable for modelling applications.

4.4 Fire risk mapping validation

To evaluate the practical applicability of the *IberFire* datacube in real-world scenarios, a fire risk mapping exercise was conducted. The objective was to assess whether the datacube features can support the generation of reliable fire risk maps when used in combination with standard machine learning techniques.

As discussed in Chapter 5, forest fires are intrinsically rare events, resulting in a highly imbalanced distribution of the `is_fire` feature, with significantly fewer fire instances relative to non-fire occurrences. To address this imbalance during model training, a balanced dataset was retrieved from *IberFire* by including all fire instances recorded between 2008 and 2023, complemented by an approximately equal number of randomly selected non-fire instances from the same dates. Due to the stochastic nature of the non-fire instance sampling, the final class counts are not exactly equal. The resulting training dataset consisted of 140,399 instances, comprising 70,476 fire cases and 69,923 non-fire cases. For each selected instance, corresponding to a unique spatio-temporal cell, all associated features were extracted from the *IberFire* datacube and stored in CSV format, with each row representing a single cell and its corresponding attributes.

Following the construction of the dataset, an XGBoost classifier was trained on the extracted instances. To reduce the risk of overfitting and ensure the generalisation capability of the model, a cross-validation strategy was implemented. After model development, an independent test set was constructed by retrieving a new balanced dataset from the *IberFire* datacube, consisting of all available fire instances from the year 2024 along with a comparable number of randomly sampled non-fire instances from the same dates. The trained model was then evaluated on this test set, yielding an Area Under the Curve (AUC) of 0.955, which indicates a high degree of predictive accuracy and robustness in real-world forecasting scenarios.

In addition to this quantitative evaluation, the classifier was used to generate daily fire risk predictions for the entire year of 2024. For each day, all corresponding spatio-temporal instances were extracted from the *IberFire* datacube and converted into CSV format to serve as input for the model. Predictions were then computed for each instance. Subsequently, the auxiliary features `x_index` and `y_index` were used to construct the daily fire risk raster maps. A selection of these predicted maps is presented in Figure 7.

Visual inspection of the resulting fire risk maps revealed a high degree of spatial and temporal coherence and alignment with historical fire incidence patterns illustrated in Figure 1. Notably, areas with historically elevated fire activity, such as Galicia, Asturias, and regions along the Portuguese

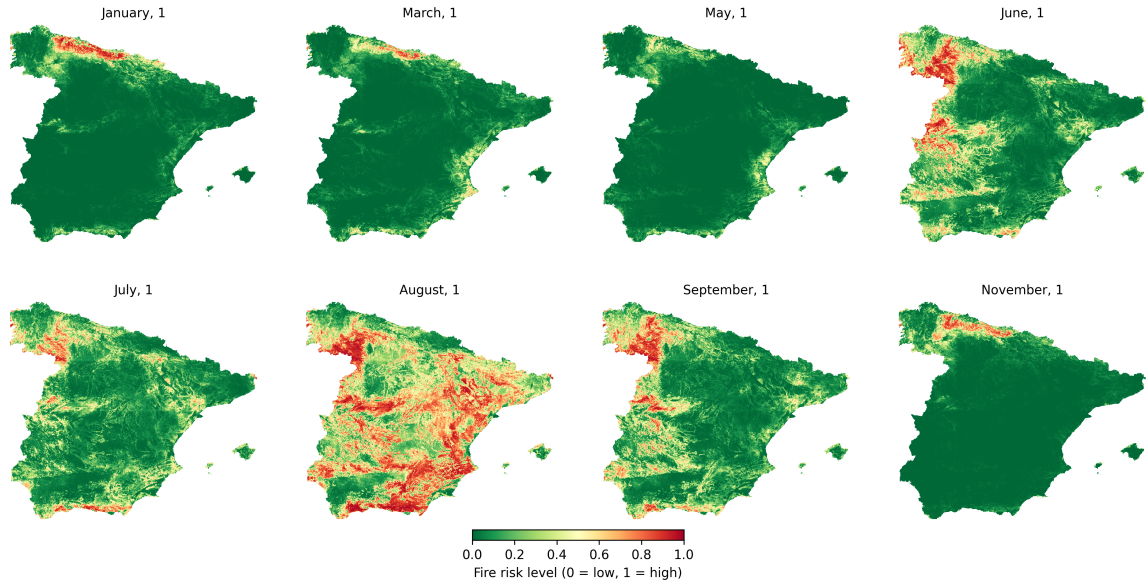


Figure 7: Forest fire risk maps for various dates of 2024.

border, consistently exhibited higher predicted risk levels, reinforcing the model’s ability to capture meaningful spatial trends in fire susceptibility. Furthermore, the model demonstrated the capability to reflect temporal variability in fire risk, with elevated predictions on dates corresponding to confirmed fire events.

These results suggest that the *IberFire* datacube serves as a reliable foundation for downstream predictive modelling and geospatial analysis. Fire risk mapping using machine learning models trained on *IberFire* can therefore be considered a promising approach for anticipating wildfire-prone areas.

5 Usage notes

The *IberFire* datacube was developed to support the modelling of wildfire occurrence risk across the Spanish territory, excluding the Canary Islands. A spatio-temporal structure was implemented to fulfil this objective, providing daily data from 01/12/2007 to 31/12/2024 over a regular grid of $1\text{km} \times 1\text{km} \times \text{spatial resolution}$. This design enables the training and validation of ML and DL models for wildfire risk prediction. The datacube is intended exclusively for mainland Spain and the Balearic Islands. To ensure that only relevant cells with complete and valid data are included in modelling workflows, users should filter the dataset accordingly using the variable `is_spain` (by selecting the instances where `is_spain = 1`).

The datacube includes daily records beginning in December 2007; however, fire occurrence data were retrieved only from 01/01/2008 onward, and all cells for December 2007 were explicitly set as non-fire. The data for December 2007 is included to enable the modelling of DL models that need multiple days of past data, like long short-term memory (LSTM) networks. Thus, even though fire predictions focus on the period from 2008 to 2024, the extended time frame ensures that models requiring temporal dependencies can be effectively trained.

Prediction targets can be defined using either the `is_fire` variable, which indicates whether a fire occurred in a given cell on a specific date, or the `is_near_fire` variable, which flags cells located in proximity to a fire event. The remaining features in the datacube are suitable for use as explanatory variables in predictive models. However, the use of the auxiliary variables `x_index` and `y_index` as model inputs is not recommended. These features were introduced to facilitate data filtering and descriptive analysis, but they lack geospatial meaning beyond the cell grid. Their values are specific to the internal indexing of the datacube and are not transferable to other geographic regions. For spatial modelling purposes, the variables `x_coordinate` and `y_coordinate`, which represent the actual projected coordinates of each grid cell on the EPSG:3035 CRS, can be used instead as they retain geographic meaning and are suitable for models requiring location-aware features.

To incorporate information about the Spanish territorial division, it is recommended to apply

one-hot encoding to the categorical `AutonomousCommunities` feature, resulting in 17 binary features corresponding to the autonomous communities listed in Table 1, excluding the Canary Islands, Ceuta, and Melilla, which are not part of the study area. Similarly, a `month` feature can be derived from the temporal coordinate of each spatio-temporal cell. As different months exhibit distinct seasonal fire risk patterns, it is also advisable to apply one-hot encoding to this variable.

It is important to note that some features, such as those derived from CLC and population density (`popdens`), are not static but are also not temporally continuous. These variables are associated with a specific year of update and thus are included in the datacube with spatial dimensions only (x, y) , rather than full spatio-temporal indices (x, y, t) . When preprocessing the datacube for modelling applications or conversion to tabular formats such as CSV or DataFrame structures, it is crucial to ensure that for each spatio-temporal cell (x, y, t) , only information available at the time t of the cell is used. For instance, when modelling a record for July 15, 2010, the appropriate population density value to use is `popdens_2010`, which should be assigned to a generic `popdens` column. Similarly, for a CLC-derived feature such as `CLC_urban_fabric_proportion`, the correct value to assign would be from `CLC_2006_urban_fabric_proportion`, since the next update in 2012 would not yet be available at that date. Careful consideration is required to prevent potential data leakage, particularly in the case of land cover features that might implicitly reflect fire occurrence. The CLC dataset contains a class representing area that was burned, which, if taken from a dataset version updated after the date being modelled, could inadvertently introduce information correlated with the target variable (`is_fire`). Such unintended inclusion of future knowledge may affect the integrity and validity of predictive modelling outcomes. When properly preprocessed, the resulting CSV dataset extracted from *IberFire* should contain a total of 145 columns, including one-hot encoded representations of month and autonomous communities.

For real-world model deployment, relying on ERA5-Land as the meteorological data source is not feasible due to its inherent 5-day latency. To address this limitation, the construction of the *IberFire* datacube was carefully designed taking into consideration operational applicability. Consequently, all meteorological features were selected and processed to align with the format and units of the open-access, near-real-time data provided by AEMET. This compatibility was validated in Section 4 through a comparison between historical AEMET measurements and the corresponding *IberFire* records. While alternative meteorological sources could be employed for model deployment instead of AEMET, doing so would require careful preprocessing to ensure compatibility with the trained models.

Class imbalance presents a significant challenge in training models for forest fire risk prediction. The proportion of positive fire instances is extremely low, as the likelihood of a specific area burning on a given day is, in general, minimal. To mitigate this imbalance during the training phase, it is advisable to construct a balanced dataset by incorporating all fire occurrences and randomly sampling an equal number of non-fire (and non near-fire) instances.

Additionally, Figure 1 displays all recorded fires during the *IberFire* study period, overlaid across the territory. As observed, some autonomous communities exhibit a significantly higher number of fire records than others. This spatial disparity may be attributed to various natural factors, such as regional climatic conditions, or anthropogenic factors, including local legislation or land management practices. Regardless of the cause, it is essential to account for this variability when designing predictive models. In certain cases, it may be advisable to develop separate models for regions sharing similar environmental or regulatory characteristics.

An essential final consideration when working with the *IberFire* datacube is the substantial computational resources required for data processing. Although the total disk size of the datacube is approximately 29GB, each spatio-temporal feature is stored in a highly compressed format. When decompressed, a single feature represented as a `float32` array occupies around 25GB of memory, making it impractical to load multiple features into RAM simultaneously on standard computing hardware. The `xarray` package handles this problem by chunking the data, and for small computations like data visualisation and analysis, standard hardware suffices. Similarly, retrieving a balanced CSV training dataset, including all fire instances and an equal number of non-fire instances, is believed to be feasible under standard memory constraints, although this has not been empirically verified on standard hardware. However, more demanding operations, such as the generation of new spatio-temporal variables derived from combinations of existing features, require significantly more memory. Therefore, all the processing steps involved in the construction of *IberFire*, including preprocessing and training dataset extraction, were executed on a machine equipped with 128GB of RAM.

6 Code Availability

The functions for loading and transforming the data were implemented in Python. The processing code used to generate the IberFire datacube, to validate it and to visualize it is available on GitHub <https://github.com/JulenErcibengoaTekniker/IberFire>.

Author Information

Authors and Affiliations

Intelligent Information Systems Unit, Tekniker, 20600, Eibar, Spain

Julen Ercibengoa, Meritxell Gómez-Omella

Department of Languages and Computer Systems, University of the Basque Country (UPV/EHU), Donostia-San Sebastián, Spain

Julen Ercibengoa, Izaro Goienetxea

Contributions

Julen Ercibengoa: Conceptualisation, Methodology, Software, Data source finding, Data retrieval, Data curation, Visualisation, Writing – original draft.

Meritxell Gómez-Omella: Conceptualisation, Project administration, Supervision Methodology, Supervision, Writing – review & editing.

Izaro Goienetxea: Conceptualisation, Supervision Methodology, Supervision, Writing – review & editing.

Corresponding Author

Correspondence to Julen Ercibengoa
julen.ercibengoa@tekniker.es

Competing Interests

The authors declare no competing interests.

Acknowledgments

This work was partly supported by GAIA project (Ref PLEC2023-010303) “Gestión integral para la prevención, extinción y reforestación debido a incendios forestales” from Spanish Research Agency (AEI).

References

- [1] Marcos Rodrigues and Juan de la Riva. An insight into machine-learning algorithms to model human-caused wildfire occurrence. *Environmental Modelling & Software*, 57:192–201, July 2014.
- [2] Sandra Oliveira, Friderike Oehler, Jesus San-Miguel-Ayanz, Andrea Camia, and Jose M. C. Pereira. Modeling spatial patterns of fire occurrence in mediterranean europe using multiple regression and random forest. *Forest Ecology and Management*, 275:117–129, July 1 2012.
- [3] Francisco Javier de Vicente y López. *Diseño de un modelo de riesgo integral de incendios forestales mediante técnicas multicriterio y su automatización en sistemas de información geográfica. Una aplicación en la comunidad valenciana*. PhD thesis, Universidad Politécnica de Madrid, 2012.
- [4] European Commission. European forest fire information system (effis). <https://forest-fire.emergency.copernicus.eu/apps/data.request.form/>, 2024. Consultado el 25 de diciembre de 2024.

- [5] Xavier Úbeda, Joaquim Farguell Pérez, Marcos Francos, and Jorge Mataix Solera. Los grandes incendios forestales y sus consecuencias en el suelo. In *Geografía: cambios, retos y adaptación: libro de actas. XVIII Congreso de la Asociación Española de Geografía, Logroño, 12 al 14 de septiembre de 2023, 2023, ISBN 978-84-09-53925-3, págs. 87-96*, pages 87–96. Asociación Española de Geografía, 2023.
- [6] C. E. Van Wagner. Structure of the canadian forest fire weather index, 1974.
- [7] Spyros Kondylatos, Ioannis Prapas, Michele Ronco, Ioannis Papoutsis, Gustau Camps-Valls, María Piles Guillem, Miguel-Ángel Fernández-Torres, and Nuno Carvalhais. Deep learning methods for daily wildfire danger forecasting. *arXiv preprint arXiv:2111.02736*, 2021.
- [8] Spyros Kondylatos, Ioannis Prapas, Michele Ronco, Ioannis Papoutsis, Gustau Camps-Valls, Maria Piles, Miguel-Angel Fernandez-Torres, and Nuno Carvalhais. Wildfire danger prediction and understanding with deep learning. *Geophysical Research Letters*, 49(17), September 16 2022.
- [9] Copernicus Land Monitoring Service. CORINE Land Cover. <https://land.copernicus.eu/en/products/corine-land-cover/clc2018Link>. Consultado el 29 de diciembre de 2024.
- [10] J. Muñoz Sabater. ERA5-Land hourly data from 1950 to present. <https://cds.climate.copernicus.eu/Link>, 2019. Consultado el 29 de diciembre de 2024.
- [11] Copernicus Land Monitoring Service. Copernicus Land Monitoring Service. <https://land.copernicus.eu/enLink>. Consultado el 29 de diciembre de 2024.
- [12] Ilektra Karasante, Lazaro Alonso, Ioannis Prapas, Akanksha Ahuja, Nuno Carvalhais, and Ioannis Papoutsis. Seasfire cube - a multivariate dataset for global wildfire modeling. *Scientific Data*, 12(1):368, 2025.
- [13] Spyros Kondylatos, Ioannis Prapas, Gustau Camps-Valls, and Ioannis Papoutsis. Mesogeos: A multi-purpose dataset for data-driven wildfire modeling in the mediterranean. In *Thirty-seventh Conference on Neural Information Processing Systems Datasets and Benchmarks Track*, 2023.
- [14] Julen Erzubengoa, Meritxell Gomez-Omella, and Izaro Goienetxea. Iberfire: a spatio-temporal dataset for wildfire risk assessment in spain. <https://doi.org/10.5281/zenodo.15225886>, April 2025.
- [15] European Space Agency. Copernicus global digital elevation model. <https://doi.org/10.5069/G9028PQBLink>, 2024. Distribuido por OpenTopography, consultado el 29 de diciembre de 2024.
- [16] WorldPop. Worldpop project. <https://www.worldpop.org/Link>, 2024. Consultado el 29 de diciembre de 2024.
- [17] OpenStreetMap contributors. Openstreetmap. <https://www.openstreetmap.orgLink>, 2024. Consultado el 29 de diciembre de 2024.
- [18] QGIS Development Team. *A Gentle Introduction to GIS: Vector Attribute Data*. QGIS Project, 2024. Accessed: 2025-04-11.
- [19] QGIS Development Team. *A Gentle Introduction to GIS: Raster Data*. QGIS Project, 2024. Accessed: 2025-04-11.
- [20] QGIS Development Team. *QGIS Geographic Information System*. Open Source Geospatial Foundation, USA, 2023. Version 3.2.
- [21] SimpleMaps. GIS Shapefiles of Spain. <https://simplemaps.com/gis/country/es>. Accessed: 2 April 2025.
- [22] European Commission. NUTS – Nomenclature of territorial units for statistics. <https://ec.europa.eu/eurostat/web/nuts>, 2016.
- [23] Área del Registro Central de Cartografía del Instituto Geográfico Nacional de España (IGN). Límites de las comunidades autónomas de España, 2018.

- [24] Helena Liz-Lopez, Javier Huertas-Tato, Jorge Perez-Aracil, Carlos Casanova-Mateo, Julia Sanz-Justo, and David Camacho. Spain on fire: A novel wildfire risk assessment model based on image satellite processing and atmospheric information. *Knowledge-Based Systems*, 283, January 11 2024.
- [25] Ministerio para la Transición Ecológica y el Reto Demográfico. Red Natura 2000: Cartografía, 2024. Accessed: 2025-04-12.
- [26] Arkadii Yakovets, Panpakorn Siripanich, and Serhii Murza. Open world holidays framework v0.70, April 2025.
- [27] Oleg A. Alduchov and Robert E. Eskridge. Improved magnus form approximation of saturation vapor pressure. *Journal of Applied Meteorology and Climatology*, 35(4):601 – 609, 1996.
- [28] World Meteorological Organization. Global climate observing system (gcos), n.d. Accessed: March 31, 2025.
- [29] W. Wagner, G. Lemoine, and H. Rott. A method for estimating soil moisture from ers scatterometer and soil data. *Remote Sensing of Environment*, 70:191–207, 1999.